Published in final edited form as:
Am J Ophthalmol. 2014 March ; 157(3): 540–549.e2. doi:10.1016/j.ajo.2013.11.007.

A Method to Estimate the Amount of Neuroretinal Rim Tissue in Glaucoma: Comparison with Current Methods for Measuring Rim Area

Stuart K Gardiner[1,*], **Ruojin Ren**[1,2], **Hongli Yang**[1], **Brad Fortune**[1], **Claude F Burgoyne**[1], and **Shaban Demirel**[1]

[1] Devers Eye Institute Legacy Research Institute 1225 NE 2nd Ave Portland, OR 97232 USA

[2] New York Eye and Ear Infirmary 310 East 14th St New York, NY 10003 USA

Abstract

Purpose—To test whether the minimum rim area assessed by spectral domain optical coherence tomography (SD-OCT), based on the shortest distance from Bruch's Membrane Opening (BMO) to the inner limiting membrane, corresponds more closely to retinal nerve fiber layer (RNFL) thickness and visual field mean deviation (MD) than current rim measures in early glaucoma.

Design—Prospective cross-sectional study.

Methods—221 participants with non-endstage glaucoma or high-risk ocular hypertension performed standard automated perimetry, and received SD-OCT and confocal scanning laser ophthalmoscopy (CSLO) scans, on the same day. Rim area measured by CSLO was compared with three SD-OCT rim measures from radial B-scans: horizontal rim area between BMO and ILM within the BMO plane; mean minimum rim width (BMO-MRW); and minimum rim area (BMO-MRA) optimized within sectors and then summed. Correlations between these measures and either MD from perimetry or RNFL thickness from SD-OCT were compared using Steiger's test.

Results—RNFL thickness was better correlated with BMO-MRA (r=0.676) or BMO-MRW (r=0.680) than with either CSLO Rim Area (r=0.330, p<0.001) or Horizontal Rim Area (r=0.482, p<0.001). MD was better correlated with BMO-MRA (r=0.534) or BMO-MRW (r=0.546) than with either CSLO Rim Area (r=0.321, p<0.001) or Horizontal Rim Area (0.403, p<0.001). The correlation between MD and RNFL thickness was r=0.646.

Conclusions—Minimum rim measurements from SD-OCT are significantly better correlated to both RNFL thickness and MD than rim measurements within the BMO plane, or based on the clinical disc margin. They provide new structural parameters for both diagnostic and research purposes in glaucoma.

* Corresponding Author Tel: +1 503 413 1199 sgardiner@deverseye.org.

C. Contributions of Authors: Design of the study (SKG, RR, HY, BF, CFB, SD), Conduct of the study (SKG, RR, HY, CFB, SD), Data collection and management (RR, HY, SD), Data analysis (SKG, RR, HY), Data interpretation (SKG, BF, CFB, SD), Manuscript preparation (SKG), Manuscript review and approval (SKG, RR, HY, BF, CFB, SD).

Introduction

Understanding the relation between structural and functional damage in glaucoma has been a key aim for many years.[1-7] For example, in the US, the National Eye Institute and Food and Drug Administration indicated that structural measures could be used as endpoints in clinical trials for glaucoma treatments if they demonstrated a strong correlation to functional measures, with $R^2 \approx 0.9$.[8] While this may seem unrealistic, better understanding of this relation would aid attempts to combine structural and functional measures to improve assessment of disease stage and progression.[9, 10] However, advances on this front have been limited by two key factors. Firstly, inter-individual variability in both structural and functional measures is considerable. The non-neural (vascular and glial) component of both the optic nerve head rim tissue and the retinal nerve fiber layer varies between individuals, and the manner in which each changes with age and disease may differ.[11] In normal healthy human eyes, there is little correlation between retinal nerve fiber layer (RNFL) thickness and contrast sensitivity,[12, 13] and in healthy eyes of non-human primates there is little correlation between RNFL thickness and total optic nerve axon count.[14] Secondly, both structural and functional tests contain significant intra-individual inter-test variability. For example, when visual field sensitivity measured with standard automated perimetry has declined to 15dB, test-retest variability is reported to have a standard deviation of up to 8dB,[15] and so the 95% confidence interval for retest sensitivity covers the majority of the perimeter's effective dynamic range. This means that even if the underlying structure-function association were perfect, its strength would be masked by this substantial variability.[16]

Much previous work has relied on performing functional testing with standard automated perimetry and structural testing with confocal scanning laser ophthalmoscopy (CSLO). Recently, Reis et al have demonstrated that CSLO does not accurately measure the neuroretinal rim area, due to the fact that important sub-surface structures are not readily identifiable on CSLO scans.[17] They showed that “the basis for current rim measurements lacks a solid anatomical foundation because (1) the clinical DM (disc margin) is not a consistent outer border of the rim tissue and (2) the orientation of neural tissue in the optic nerve head is not accounted for.”[18] This could be a significant contributing factor to the variability of the structure-function relation when structure is assessed using CSLO. Improving the structure-function relation therefore requires new and improved testing methodologies that have a stronger link to anatomy and hence lower variability, for structural as well as functional testing.

Recently, optical coherence tomography (OCT) has been developed. It has been widely used to measure RNFL thickness at a specific angular eccentricity from the center of the optic disc. The RNFL thickness and retinal nerve fiber layer cross-sectional area measures from CSLO are sub-optimal, since they are based on the vertical distance between the tomographically-determined retinal height and a reference plane, and hence are actually measures of relative height rather than the true thickness of any retinal layer. By contrast, the RNFL thickness measure is derived as the distance between the anterior and posterior borders of the highly reflective nerve fiber layer, and so should better reflect the targeted anatomy.

OCT can also be used to perform scans through the optic nerve head. OCT reveals sub-surface structures that are not evident using previous techniques such as CSLO or stereophotography. Time-domain OCT has been shown to improve the correlation between global RNFL thickness and functional measures from 0.33 (using CSLO) to 0.48 (using OCT).[19] The more recent development of spectral-domain OCT (SD-OCT) could improve this relation even further, given its greater axial resolution and that its faster speeds can

reduce motion artifact within denser scan patterns. Better methods to quantify SD-OCT images are being developed. Povazay et al suggested that 'rim' could be better defined as the area of a surface extending from Bruch's Membrane Opening (BMO) to the Inner Limiting Membrane.[20] Strouthidis et al demonstrated using SD-OCT that this rim parameter was both reliable and sensitive in a longitudinal study of non-human primates with experimental glaucoma[21] and in studies of acute intraocular pressure elevation.[22] Reis et al also measured this using SD-OCT, and showed that it reflected the anatomy of the optic nerve head better than the clinically-visible "disc margin".[18] This would prevent the problem above whereby current clinical measurements of the rim were not consistently referenced to any given anatomical structure.[23] By removing this large source of anatomic variability, this type of SD-OCT-based assessment of the neuroretinal rim should be more comparable between individuals, improving the ability to detect the presence of glaucomatous damage[24] and its progression.

Different variants of neuroretinal rim assessment are considered in this paper, as detailed in the Methods section. Firstly, a horizontal rim area measurement is considered, giving the most direct analogous measurement to current rim assessment. For example, this is the same as the method used by the Cirrus SD-OCT instrument (Carl Zeiss Meditec, Dublin, CA, USA) to generate a "rim area" measurement.[25, 26] Secondly, a mean minimum rim width measurement from BMO (BMOMRW) is considered, along an angle that varies between radial scans in order to represent the minimum distance from the BMO to the Inner Limiting Membrane within each radial scan around the optic nerve head rim, similar to the technique proposed by Povazay et al [20] and Chen.[27] Unlike the 'clinical disc margin', BMO is an actual anatomic boundary of the neuroretinal rim tissue. BMO-MRW therefore represents an accurate estimate of the minimum width of the neural tissues relative to each BMO point within the plane of each radial B-scan. Finally, this minimum rim width is used to estimate the minimum rim area (BMO-MRA) through which the axons must pass. This adjusts for the fact that the BMO-MRW will be related to disc size and not just the number of axons.

This study compares current, disc margin based rim area measurements from CSLO with these new, BMO based measurements from SD-OCT.[17, 18] The starting point for the comparison is the principle that a sound measure of neuroretinal rim should correlate well with RNFL thickness (since the same axons comprise both), and with function (since glaucomatous loss of RNFL thickness is associated with concomitant loss of function). The paper aims first to determine whether horizontal or minimum measurements of the rim based on BMO as assessed by SD-OCT are better correlated with RNFL thickness than the current rim area measure from CSLO. Second, the paper aims to determine whether these new measures of optic nerve head neuroretinal rim tissue also result in a stronger correlation between visual field mean deviation (MD) and optic disc rim structure.

Methods

Participants

Data from 221 participants with non-endstage glaucoma (i.e. with remaining measureable visual function), or with ocular hypertension plus risk factors for glaucoma were taken from the ongoing Portland Progression Project, a prospective study of the course and risk factors for glaucomatous progression.[28] All protocols were approved and monitored by the Legacy Health Institutional Review Board, and adhere to the Health Insurance Portability and Accountability Act of 1996 and the tenets of the declaration of Helsinki. All participants provided written informed consent for their participation in the study once all of the risks and benefits of their involvement were explained to them.

At study entry, participants either had a clinical diagnosis of early glaucoma, or they had ocular hypertension (untreated IOP greater than 22mmHg) and their physician had determined that they had glaucomatous optic neuropathy and/or suspicious optic nerve head appearance (cup-disc ratio asymmetry > 0.2, neuroretinal rim notching or narrowing, disc hemorrhage) and/or one or more other risk factors for glaucoma (e.g. age > 70, systemic hypertension, migraine, diet controlled diabetes, peripheral vasospasm, African ancestry or self-reported family history of glaucoma).[6, 29] Participants were excluded if they had other factors (diseases and/or medications) likely to affect the visual field, or if they had undergone ocular surgery (except for uncomplicated cataract surgery). Eyes with visual acuity worse than 20/40 were also excluded, aiming to remove participants with worse than mild media change or cataract.

Testing Protocol

Participants underwent functional testing using standard automated perimetry, structural testing using CSLO, stereo optic disc photography (3-Dx; Nidek Co., Gamagori, Japan), and structural testing using SD-OCT, all on the same day. Demographic data and intraocular pressure were also recorded. Data were used from the earliest visit at which testing was carried out and reliable results (as defined below) were obtained for all three tests. When suitable data were available for both eyes of a participant, the eye with the better quality SD-OCT scan was chosen, or one eye was arbitrarily chosen if these were equal.

Visual field testing was performed using a Humphrey Field Analyzer II (Carl Zeiss Meditec Inc, Dublin, CA, USA), employing the 24-2 testing pattern and conventional test procedures.[30] The SITA standard algorithm [31] was used for all testing. An optimal lens correction was placed before the tested eye, and the fellow eye was occluded with a white plastic eye patch. All participants had previous experience with visual field testing prior to entering the study, and most had undergone multiple previous tests. Only reliable tests were included, defined as ≤33% false negatives and ≤15% false positives, and either ≤20% fixation losses or confirmation from the monitoring technician that eye position remained stable throughout the test (since fixation losses can be erroneously reported when the perimeter's initial automated mapping of the blind spot is inaccurate). The Mean Deviation index (MD) was used to characterize the degree of functional damage.

CSLO optic nerve head scanning was performed using a Heidelberg Retina Tomograph Classic (Heidelberg Engineering, GmbH, Heidelberg, Germany) following standard operating procedures.[32] Scans of acceptable quality as judged by the experienced operator were included. The topography standard deviation was always better than 40μm. The disc margin was marked by an experienced clinician (author CFB) guided by stereophotographs that were acquired on the same day. The CSLO neuroretinal rim area was generated using the instrument's standard reference plane, defined as 50 microns below the average topography value at positions between 350° to 356° on the marked disc margin.

Standard SD-OCT imaging was performed using a Heidelberg Spectralis (Heidelberg Engineering, GmbH, Heidelberg, Germany) with a 870nm light source. All SD-OCT datasets had a quality score above 15. A peripapillary circle scan with a fixed 6° radius centered on the optic nerve head was performed, and the automated delineation of the resulting image was examined and refined by experienced technicians. This was used to calculate the average RNFL thickness measurement. 48 radial B-scans centered on the optic nerve head were also captured, and a subset of 24 (every alternate B-scan) were manually delineated using custom Multiview software by a single delineator for each eye (one of two delineators for the entire dataset)[21] to determine the positions of the Inner Limiting Membrane and Bruch's Membrane opening (BMO), as seen in Figure 1. These delineated

landmarks were combined to provide a three-dimensional representation of the Inner Limiting Membrane and BMO. Neuroretinal rim measurements were then calculated.

Optical Coherence Tomography Parameterization

The horizontal rim area was designed to conceptually resemble the parameter CSLO Rim Area and current SD-OCT rim assessment, and most closely mimic a clinician's rim assessment. It was based on the distance from the BMO to the Inner Limiting Membrane along the plane of the BMO within each radial B-scan ("horizontal"), as indicated by the green arrows in Figure 1. This gives 48 horizontal rim width measurements[18] (two for each of the 24 delineated B-scans). For each of these measurements, the corresponding area was calculated using a circular section of width 7.5° and appropriate diameter *r* (based on the distance from the BMO centroid to the BMO in that radial B-scan), as shown by the green outline in Figure 1. Specifically, the sectoral horizontal rim area equals the difference between the areas of two 7.5° circular sectors, one of radi us *r* and one of radius (*r* - horizontal rim width). These sectoral areas were added to give the overall Horizontal Rim Area measure. For eyes in which the cup was so shallow that the Inner Limiting Membrane never crossed the plane of the BMO, the Horizontal Rim Area was set to equal the entire area enclosed by the BMO. This measure is similar to the Rim Area measure produced by the Cirrus SD-OCT research software, which performs the same calculation using a reference plane 200μm anterior to the BMO.[33] BMO points from locations around the optic nerve head will generally not all lay within a single plane (unlike the single depth used to define the CSLO "reference plane"), but instead form a 3-dimensional elliptical ring with varying axial depth.

The mean minimum rim width (BMO-MRW) was based on the distance from the delineated BMO point to the closest point on the Inner Limiting Membrane within each radial B-scan, as first described by Povazay et al,[20] and as indicated by the yellow arrows in Figure 2. This minimum will occur at an angle θ to the BMO plane (as marked in blue) that can vary between the different radial scans in a given eye. Note that this represents the minimum rim width from each delineated BMO point within one side of the radial B-scan,[18] within the plane of the acquired B-scan rather than the global minimum distance to the Inner Limiting Membrane from that BMO location (which would require interpolation of the Inner Limiting Membrane surface between the available B-scans). These rim widths were then averaged across sectors to give the global measure BMO-MRW.

The motivation for assessing this minimum distance is that it approximates the smallest cross-sectional area through which nerve fibers must pass en route from the retina to the optic nerve for a particular part of the optic nerve head. However, it does not provide a true surrogate measure for the number of axons, since the same BMO-MRW would correspond to a larger cross-sectional area in eyes with larger discs. Thus, the number of axons would likely better correlate with the minimum cross-sectional area (BMO-MRA) through which the axons pass than with BMO-MRW.

BMO-MRA was estimated as the sum of the areas of 48 trapeziums, each extending from a delineated BMO point to the Inner Limiting Membrane at angle ϕ above the BMO plane, as indicated by the yellow outlines in Figure 2. One such trapezium is associated with each delineated BMO point, defined as being at radius *r* from the BMO centroid. The base of the trapezium then extends halfway to the adjacent radials, and so has length $2\pi r/48$. The height of the trapezium is set to equal the rim width at angle ϕ above the BMO plane in that radial, RW_ϕ, as shown by the yellow arrows in Figure 2. The top of the trapezium is then at horizontal distance $(r - RW_\phi*\cos(\phi))$ from the BMO centroid. This means that the length of the top is given by $2\pi r/48*(r - RW_\phi*\cos(\phi))$. Within each radial, the angle ϕ was optimized to give the smallest rim area. This means that ϕ does not necessarily equal θ, the angle of the

MRW measurement. They are shown as being the same in Figure 2 for simplicity. For example, consider the case where the rim width perpendicular to the BMO plane (i.e. ϕ=90°) is 100μm, and the width parallel to the BMO plane (i.e. ϕ=0°) is 105μm, with radius r=1000μm. The corresponding sectoral area from the above formulae measured perpendicular to the BMO plane is then 13090μm^2, whereas the area parallel to the BMO plane is 13023μm^2. In this example, this sector's contribution to BMO-MRW would be measured at θ=90°, whereas for BMO-MRA it would be measured at ϕ=0°. θ is chosen to minimize the rim width, whereas ϕ is chosen to minimize the rim area. Supplementary Figure S1 shows a demonstration of this in schematic form. The areas of the sectoral trapeziums were calculated based on these dimensions, and added together to give the global minimum rim area measure BMO-MRA. Unlike the Horizontal Rim Area above, these minimum rim measures are not affected by the possibility that the cup may not break than the BMO plane.

The relation between the mean RNFL thickness and the corresponding cross-sectional area does not depend on the disc circumference, with one being a multiple of the other. Even though we report an RNFL thickness measure, it can be treated the same as an area measure, in particular allowing the relation between RNFL thickness and rim area to be modeled using a linear fit. We chose to use RNFL thickness because it has been more commonly used in the literature, whether using temporal domain or (as in this study) spectral domain OCT.

Data Analysis

The primary outcome measures were the correlations between each of the neuroretinal rim measures (CSLO Rim Area, Horizontal Rim Area, BMO-MRW, and BMO-MRA) and either RNFL thickness or function (MD). Pearson correlations were used, and were compared using Steiger's Z_2* test for non-independent data.

It has been suggested that structure and function are better correlated when the functional measures are expressed on a linear, rather than logarithmic (dB) scale.[4, 11, 12, 34, 35] Therefore this analysis was repeated after transforming the functional data onto a linear scale proportional to 1/Contrast. To achieve this, pointwise total deviation values (TD) were converted to $10^{TD/10}$, and then these values averaged to give the index Linearized MD. We have previously reported that this transformation may exaggerate variability at locations with above-normal sensitivities.[36] Therefore, another index was calculated in the same manner after first capping all Total Deviation values at zero, Capped Linearized MD = mean($10^{\min(TD, 0)/10}$).

Results

Reliable data, with all four testing methods (standard automated perimetry, CSLO, stereophotographs and SD-OCT) performed on the same day, were available for 221 eyes of 221 participants. Their demographic and clinical characteristics are summarized in Table 1. 38 eyes had MD outside normal limits, and 43 had abnormal pattern standard deviation. 143 eyes had BMO-MRW below the normative limits (275.4 – 361.7μm) given by Chauhan et al.[24]

Table 2 shows the correlations between each rim area measure and the four outcome variables. All correlations were significant ($p<0.001$ in all cases). The correlations with either BMO-MRW or BMOMRA were significantly stronger than those with CSLO Rim Area for all outcome variables ($p<0.004$ in all cases). Correlations with Horizontal Rim Area were also greater than those with CSLO Rim Area for all measures, but this difference was not always significant (MD p=0.141; Linearized MD p=0.399; Capped Linearized MD p=0.222; RNFL thickness p=0.003). Correlations with Horizontal Rim Area were

significantly weaker than those with BMO-MRW (MD p=0.001; Linearized MD p=0.010; Capped Linearized MD p=0.007; RNFL thickness p<0.001) or with BMO-MRA (MD p<0.001; Linearized MD p=0.001; Capped Linearized MD p<0.001; RNFL thickness p<0.001). Figure 3 shows the relations between CSLO Rim Area or BMO-MRA with MD or RNFL thickness. While the patterns are similar, the relation clearly has more scatter when using CSLO Rim Area (left panels) than when using BMO-MRA (right panels).

The two parameters BMO-MRW and BMO-MRA both gave higher correlations with MD and RNFL thickness than the other rim area parameters. There were no significant differences between BMOMRW and BMO-MRA for predicting RNFL thickness (p=0.893) or MD (p=0.720). Notably, MD was better correlated with RNFL thickness (Correlation=0.646) than with either BMO-MRW (p=0.027) or BMO-MRA (p=0.015).

The functional metric MD is age corrected, whereas the RNFL thickness and rim area measures are not. However, this did not make any appreciable difference to the results. When MD was predicted by age and RNFL thickness together, age was not a significant predictor (p=0.415). Similarly, age was not a significant predictor when included in bivariate models to predict MD with BMO-MRW (p=0.556) or BMO-MRA (p=0.820). In part, this may be because changes in the RNFL thickness and visual field sensitivity due to glaucoma are far greater than those due to aging.

Discussion

This study agrees with previous results suggesting that the rim area CSLO Rim Area measured using CSLO does not correlate particularly well with either RNFL thickness measured by SD-OCT or with function in patients with ocular hypertension or non-endstage glaucoma.[19] This could be in part a consequence of the fact that the measure CSLO Rim Area is based on the clinical disc margin and measured “horizontally” within an arbitrary reference plane that is a fixed distance beneath the plane of the peripapillary retinal surface, and thus, does not accurately reflect the true amount of rim tissue.[17, 18, 23] The most direct comparison between SD-OCT and CSLO rim measures is the comparison of the Horizontal Rim Area to CSLO Rim Area, since both are based on “horizontal” rather than minimum measurements of the rim. Horizontal Rim Area is currently the most commonly used method employed within commercial OCT instruments, similar to the output from the Cirrus SD-OCT instrument that is labeled “Rim Area”. The correlation between Horizontal Rim Area and RNFL thickness was greater than that between CSLO Rim Area and RNFL thickness, and similarly for correlations with MD, indicating that the structure-function relation is strengthened by using rim measurements based on BMO (SD-OCT) rather than on the ‘clinical disc margin’ (CSLO).

However, a horizontal measurement made from BMO or from the clinical disc margin does not account for the axons’ trajectories. By contrast, BMO-MRW and its associated area measure BMO-MRA are based on measurements approximately perpendicular to the greatest proportion of axons. This therefore reduces variability compared with Horizontal Rim Area, which is measured along a line through which axons pass at an angle that will vary significantly both between and within eyes. As a result, SD-OCT BMO-MRW and BMO-MRA were both significantly better correlated with both RNFL thickness and function than either Horizontal Rim Area or CSLO Rim Area. Our data suggest that BMOMRA and BMO-MRW provide good surrogate measures for the number of axons entering the optic nerve head, and so should be considered for studies of optic nerve head structure and visual function. Of note, BMO-MRA and BMO-MRW cannot be assessed by ophthalmoscopy alone, but require three-dimensional imaging of the neuroretinal rim such as that provided by SD-OCT.[23] In the medium term, better algorithms will be developed to

produce more accurate measures of the true minimum rim area in particular, and the correlations with RNFL thickness and MD should improve slightly.

Conceptually, the minimum rim area should represent the smallest area through which the nerve fiber bundles must pass. However, this area could be defined either by the BMO or by the anterior scleral canal opening, or some combination of both. In some eyes, the neural retina (outer and inner nuclear layers) extends beyond the BMO in certain sectors, which may impose further limits on the minimum passage. However, the anterior scleral canal opening is not yet consistently visible on SD-OCT scans and automated segmentation algorithms can more readily identify the BMO than the end of the retinal nuclear layers. While we refer to the parameter as BMO-MRA, it should be acknowledged that it might not represent the true absolute minimum rim area. It is the rim area relative to BMO, which is chosen because it is a structure that is consistently visible within SD-OCT images from the majority of human eyes.

It is apparent from the results of this study that MD is better correlated with the measure RNFL thickness than with any of the rim measurements. The correlation with MD was greater using RNFL thickness than the best performing rim measure BMO-MRW (comparison p=0.027). However, a recent study by Nilforushan et al suggested in contrast that MD correlated better with rim area (from the Cirrus SD-OCT) than RNFL thickness,[37] and Chauhan et al have reported that BMO-MRW is better than RNFL thickness for detecting open-angle glaucoma.[24] It may be that blood vessels, outer retinal and glial components of the rim have a proportionately larger effect on rim area estimates than on RNFL thickness measured at 6° eccentricity from the cent er of the optic nerve head. If this is true, better algorithms to identify and isolate these non RGC axon rim components should lead to more accurate neural rim tissue estimates that further improve correlations with RNFL thickness and visual field MD. Deformation of optic nerve head connective tissue structure during acute IOP elevation and after chronic IOP elevation in non-human primates also influences the BMO-MRW and BMO-MRA parameters to a much greater extent than it influences peripapillary RNFL thickness.[21, 22] It is plausible that these issues will be resolved by examining correlations between longitudinal changes in structure and function.

Blood vessels will also likely have a proportionately larger effect on rim area than on rim width. If the presence of a blood vessel increases the rim width in a given sector by 10%, then it will increase the area by 21%. Even though there was little difference between the performance of the rim width and rim area parameters in this study, area measures may provide greater benefits once blood vessels and other components of the rim tissue can be removed from the calculation.

As seen in Figure 3, the relations between rim area and MD appear to be non-linear, as would be expected based on previous literature.[11, 12, 34, 35, 38] However, the perimetric testing algorithms are designed to minimize errors on a dB scale rather than a linear scale, and so the inter-test variability of perimetry is greater when transformed to a linear scale.[36] Therefore, the structure-function correlations are currently no better when using linearized indices such as Linearized MD or Capped Linearized MD than when using MD. This could change with the development of linear-scale optimized thresholding algorithms.

The best structure-function relation seen in this study was that between MD and RNFL thickness, with R^2=0.42. This is a long way from the aim of a relation with $R^2 \approx 0.9$ to enable structural endpoints to be used as the sole outcome measure in clinical trials, as set out by the National Eye Institute and Food and Drug Administration.[8] Given the variability in the structure-function relation among normal subjects,[12, 13] and the high variability of both measures ($R^2 \approx 0.9$ would be unlikely even between two functional tests carried out on

the same day), it seems unlikely that any cross-sectional study could result in a correlation of that strength. The structure-function correlation may be further improved by future developments in structural and (in particular) functional testing. It could also be increased by extending the range of disease severities used. Our cohort contained a large proportion of eyes that were within normal limits for other functional and/or structural parameters. It is also possible that the structure-function correlation could be improved by weighting the rim or retinal nerve fiber layer measures based on the position around the optic nerve head, since only more central regions of the visual field are sampled by the 24-2 grid of test locations, whereas the structural measures that were used weight the entire circumference of the optic nerve head equally. This issue was not examined in this study, since the optimal weighting would vary between measurements (based in part on the distance of the measurement from the center of the optic nerve head), confounding direct comparisons between the structural measures. Finally, it may be that significantly stronger correlations can only be achieved by examining the relation between rates of structural and functional change, as this could remove much of the normal inter-individual variability (although such correlations would be limited by the range of rates of change available in the cohort).

In a clinical setting the OCT scan quality matters and every effort should be made to maximize scan quality. It is not yet known which parameters are most robust to this issue, and the longitudinal signal-to-noise ratios are not yet available. All parameters derived from scans with very poor quality should be treated with caution, as this may result in unreliability of automated segmentation algorithms.[39, 40]

In summary, the minimum rim estimates from SD-OCT were significantly better related to both RNFL thickness and functional measures than the rim area measure from CSLO, approximately doubling the correlations observed. This is likely because these measures more accurately reflect the true anatomy of the optic nerve head, and so correspond closer to the number of axons entering the optic nerve. These SD-OCT minimum rim measures should be considered as structural measures for both diagnostic and research purposes in glaucoma.

Supplementary Material

Refer to Web version on PubMed Central for supplementary material.

Acknowledgments

A. Funding: NIH R01-EY19674 (to author SD); NIH R01-EY021281 (to author CFB); The Legacy Good Samaritan Foundation, Portland, OR. The sponsors / funding organizations had no role in the design or conduct of this research.

B. Financial Disclosures: Dr. Gardiner has acted as a consultant for Allergan Inc. Dr. Burgoyne receives equipment and unrestricted research support from Heidelberg Engineering for whom he is a consultant. In addition he receives occasional travel expenses, but no speaking honoraria or personal income. Dr. Demirel has received travel expenses from Heidelberg Engineering and was site PI in a clinical trial that utilized the Spectralis OCT. He has also received no-cost software licenses that allow extraction of visual field data from the Humphrey Visual Field Analyzer from Carl Zeiss Meditec.

D. No other acknowledgements are relevant for this study.

Biography

References

1. Caprioli J. Correlation of visual function with optic nerve and nerve fiber layer structure in glaucoma. Surv Ophthalmol. 1989; 33(S):319–30. [PubMed: 2655145]
2. Anton A, Yamagishi N, Zangwill L, Sample PA, Weinreb RN. Mapping structural to functional damage in glaucoma with standard automated perimetry and confocal scanning laser ophthalmoscopy. Am J Ophthalmol. 1998; 125(4):436–446. [PubMed: 9559728]
3. Garway-Heath D, Holder G, Fitzke F, Hitchings R. Relationship between Electrophysiological, Psychophysical, and Anatomical Measurements in Glaucoma. Invest Ophthalmol Vis Sci. 2002; 43(7):2213–2220. [PubMed: 12091419]
4. Harwerth R, Carter-Dawson L, Smith E, Barnes G, Holt W, Crawford M. Neural Losses Correlated with Visual Losses in Clinical Perimetry. Invest Ophthalmol Vis Sci. 2004; 45(9):3152–3160. [PubMed: 15326134]
5. Schlottmann P, De Cilla S, Greenfield D, Caprioli J, Garway-Heath D. Relationship between Visual Field Sensitivity and Retinal Nerve Fiber Layer Thickness as Measured by Scanning Laser Polarimetry. Invest Ophthalmol Vis Sci. 2004; 45(6):1823–1829. [PubMed: 15161846]
6. Gardiner SK, Johnson CA, Cioffi GA. Evaluation of the Structure-Function Relationship in Glaucoma. Invest Ophthalmol Vis Sci. 2005; 46(10):3712–3717. [PubMed: 16186353]
7. Anderson R. The psychophysics of glaucoma: improving the structure/function relationship. Prog Retin Eye Res. 2006; 25(1):79–97. [PubMed: 16081311]
8. Weinreb RN, Kaufman PL. Glaucoma Research Community and FDA Look to the Future, II: NEI/FDA Glaucoma Clinical Trial Design and Endpoints Symposium: Measures of Structural Change and Visual Function. Invest Ophthalmol Vis Sci. 2011; 52(11):7842–7851. [PubMed: 21972262]
9. Shah NN, Bowd C, Medeiros FA, et al. Combining Structural and Functional Testing for Detection of Glaucoma. Ophthalmology. 2006; 113(9):1593–1602. [PubMed: 16949444]
10. Medeiros FA, Zangwill LM, Girkin CA, Liebmann JM, Weinreb RN. Combining Structural and Functional Measurements to Improve Estimates of Rates of Glaucomatous Progression. Am J Ophthalmol. 2012; 153(6):1197–1205. [PubMed: 22317914]
11. Harwerth RS, Wheat JL, Fredette MJ, Anderson DR. Linking structure and function in glaucoma. Prog Retin Eye Res. 2010; 29(4):249–271. [PubMed: 20226873]
12. Hood D, Anderson S, Wall M, Kardon R. Structure versus Function in Glaucoma: An Application of a Linear Model. Invest Ophthalmol Vis Sci. 2007; 48(8):3662–3668. [PubMed: 17652736]
13. Hood DC, Anderson SC, Wall M, Raza AS, Kardon RH. A Test of a Linear Model of Glaucomatous Structure-Function Loss Reveals Sources of Variability in Retinal Nerve Fiber and Visual Field Measurements. Invest Ophthalmol Vis Sci. 2009; 50(9):4254–4266. [PubMed: 19443710]
14. Cull GA, Reynaud J, Wang L, Cioffi GA, Burgoyne CF, Fortune B. Relationship between Orbital Optic Nerve Axon Counts and Retinal Nerve Fiber Layer Thickness Measured by Spectral Domain Optical Coherence Tomography. Invest Ophthalmol Vis Sci. 2012; 53(12):7766–7773. [PubMed: 23125332]
15. Henson D, Chaudry S, Artes P, Faragher E, Ansons A. Response variability in the visual field: comparison of optic neuritis, glaucoma, ocular hypertension, and normal eyes. Invest Ophthalmol Vis Sci. 2000; 41(2):417–421. [PubMed: 10670471]

16. Gardiner S, Johnson C, Demirel S. The effect of test variability on the structure–function relationship in early glaucoma. Graefes Arch Clin Exp Ophthalmol. 2012; 250(12):1851–1861. [PubMed: 22527311]

17. Reis ASC, Sharpe GP, Yang H, Nicolela MT, Burgoyne CF, Chauhan BC. Optic Disc Margin Anatomy in Patients with Glaucoma and Normal Controls with Spectral Domain Optical Coherence Tomography. Ophthalmology. 2012; 119(4):738–747. [PubMed: 22222150]

18. Reis ASC, O'Leary N, Yang H, et al. Influence of Clinically Invisible, but Optical Coherence Tomography Detected, Optic Disc Margin Anatomy on Neuroretinal Rim Evaluation. Invest Ophthalmol Vis Sci. 2012; 53(4):1852–1860. [PubMed: 22410561]

19. Bowd C, Zangwill L, Medeiros F, et al. Structure-Function Relationships Using Confocal Scanning Laser Ophthalmoscopy, Optical Coherence Tomography, and Scanning Laser Polarimetry. Invest Ophthalmol Vis Sci. 2006; 47(7):2889–2895. [PubMed: 16799030]

20. Povazay B, Hofer B, Hermann B, et al. Minimum distance mapping using three-dimensional optical coherence tomography for glaucoma diagnosis. J Biomed Opt. 2007; 12(4):041204–8. [PubMed: 17867793]

21. Strouthidis NG, Fortune B, Yang H, Sigal IA, Burgoyne CF. Longitudinal Change Detected by Spectral Domain Optical Coherence Tomography in the Optic Nerve Head and Peripapillary Retina in Experimental Glaucoma. Invest Ophthalmol Vis Sci. 2011; 52(3):1206–1219. [PubMed: 21217108]

22. Strouthidis NG, Fortune B, Yang H, Sigal IA, Burgoyne CF. Effect of Acute Intraocular Pressure Elevation on the Monkey Optic Nerve Head as Detected by Spectral Domain Optical Coherence Tomography. Invest Ophthalmol Vis Sci. 2011; 52(13):9431–9437. [PubMed: 22058335]

23. Chauhan BC, Burgoyne CF. From Clinical Examination of the Optic Disc to Clinical Assessment of the Optic Nerve Head: A Paradigm Change. Am J Ophthalmol. 2013; 156(2):218–227. [PubMed: 23768651]

24. Chauhan BC, O'Leary N, AlMobarak FA, et al. Enhanced Detection of Open-angle Glaucoma with an Anatomically Accurate Optical Coherence Tomography-Derived Neuroretinal Rim Parameter. Ophthalmology. 2013; 120(3):535–543. [PubMed: 23265804]

25. Abràmoff MD, Lee K, Niemeijer M, et al. Automated Segmentation of the Cup and Rim from Spectral Domain OCT of the Optic Nerve Head. Invest Ophthalmol Vis Sci. 2009; 50(12):5778–5784. [PubMed: 19608531]

26. Mwanza J-C, Oakley JD, Budenz DL, Anderson DR. Ability of Cirrus HD-OCT Optic Nerve Head Parameters to Discriminate Normal from Glaucomatous Eyes. Ophthalmology. 2011; 118(2):241–248. e1. [PubMed: 20920824]

27. Chen T. Spectral Domain Optical Coherence Tomography in Glaucoma: Qualitative and Quantitative Analysis of the Optic Nerve Head and Retinal Nerve Fiber Layer (An AOS Thesis). Trans Am Ophthalmol Soc. 2009; 107:254–281. [PubMed: 20126502]

28. Gardiner SK, Johnson CA, Demirel S. Factors predicting the rate of functional progression in early and suspected glaucoma. Invest Ophthalmol Vis Sci. 2012; 53(7):3598–3604. [PubMed: 22570353]

29. Spry P, Johnson C, Mansberger S, Cioffi G. Psychophysical investigation of ganglion cell loss in early glaucoma. J Glaucoma. 2005; 14(1):11–18. [PubMed: 15650598]

30. Anderson, D.; Patella, V. Automated Static Perimetry. 2 ed.. Mosby; St. Louis, MO: 1999. p. 147-159.

31. Bengtsson B, Olsson J, Heijl A, Rootzen H. A new generation of algorithms for computerized threshold perimetry, SITA. Acta Ophthalmol. 1997; 75(4):368–375.

32. Fingeret, M.; Flanagan, J.; Lieberman, J., editors. The Heidelberg Retina Tomograph II Primer. Heidelberg Engineering; Heidelberg, Germany: 2005.

33. Moghimi S, Hosseini H, Riddle J, et al. Measurement of Optic Disc Size and Rim Area with Spectral-Domain OCT and Scanning Laser Ophthalmoscopy. Invest Ophthalmol Vis Sci. 2012; 53(8):4519–30. [PubMed: 22577077]

34. Garway-Heath D, Caprioli J, Fitzke F, Hitchings R. Scaling the hill of vision: the physiological relationship between light sensitivity and ganglion cell numbers. Invest Ophthalmol Vis Sci. 2000; 41(7):1774–1782. [PubMed: 10845598]

35. Hood D, Kardon R. A framework for comparing structural and functional measures of glaucomatous damage. Prog Retin Eye Res. 2007; 26(6):688–710. [PubMed: 17889587]

36. Gardiner SK, Demirel S, Johnson CA, Swanson WH. Assessment of linear-scale indices for perimetry in terms of progression in early glaucoma. Vision Res. 2011; 51(16):1801–1810. [PubMed: 21704057]

37. Nilforushan N, Nassiri N, Moghimi S, et al. Structure-Function Relationships between Spectral-Domain OCT and Standard Achromatic Perimetry. Invest Ophthalmol Vis Sci. 2012; 53(6):2740–2748. [PubMed: 22447869]

38. Harwerth R, Quigley H. Visual Field Defects and Retinal Ganglion Cell Losses in Patients With Glaucoma. Arch Ophthalmol. 2006; 124(6):853–859. [PubMed: 16769839]

39. Cheung CYL, Leung CKS, Lin D, Pang C-P, Lam DSC. Relationship between Retinal Nerve Fiber Layer Measurement and Signal Strength in Optical Coherence Tomography. Ophthalmology. 2008; 115(8):1347–1351. [PubMed: 18294689]

40. Folio LS, Wollstein G, Ishikawa H, et al. Variation in optical coherence tomography signal quality as an indicator of retinal nerve fibre layer segmentation error. Br J Ophthalmol. 2012; 96(4):514–518. [PubMed: 21900227]

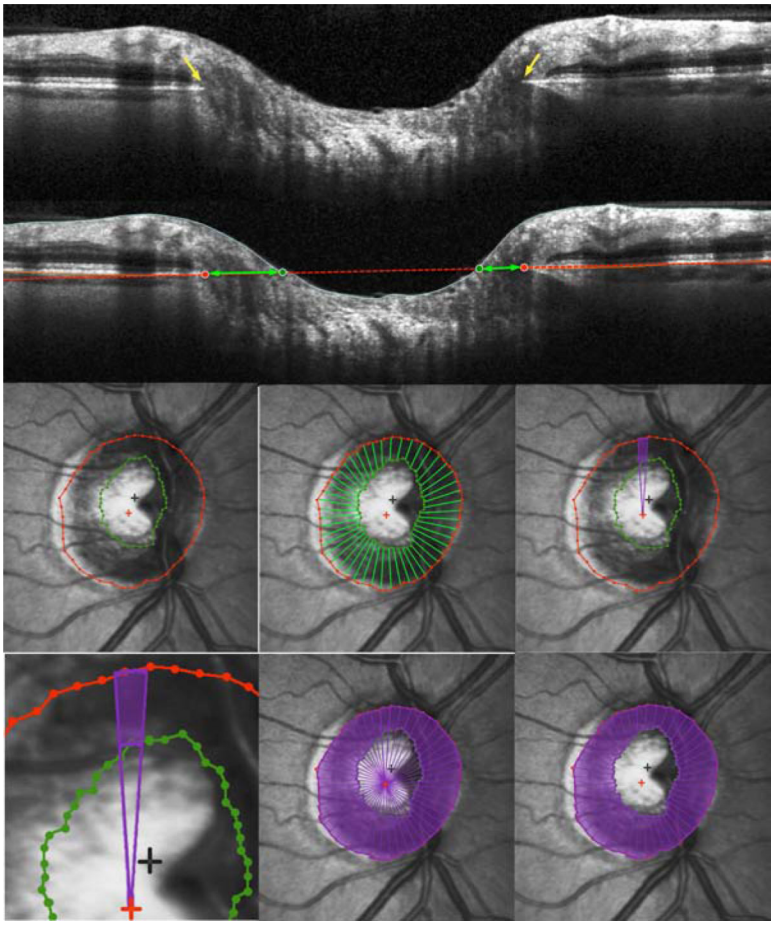

Figure 1. Definition and calculation of Bruch's Membrane Opening Horizontal Rim Area, as used to Estimate the Amount of Neuroretinal Rim Tissue in Glaucoma

(Top) Within each of the 24 radial scans, Bruch's Membrane Opening was delineated, shown by yellow arrows. (Second Panel) A plane was then fit to these 48 points, shown in red. Its intersection with the inner limiting membrane within each B-scan was marked (green circles). (Third Row, from left) Bruch's Membrane Opening (red) and Inner Limiting Membrane (green) intersection points were fit using B-splines and projected onto the plane. 48 radial interpolated horizontal rim widths (green lines) were interpolated from the Bruch's Membrane Opening centroid (red cross) at 7.5° intervals. For each 7.5° degree interval, the sectoral rim are a (purple) was calculated as the difference between areas of two circular sectors. (Bottom Row) Bruch's Membrane Opening Horizontal Rim Area was generated by summing these 48 sectoral areas.

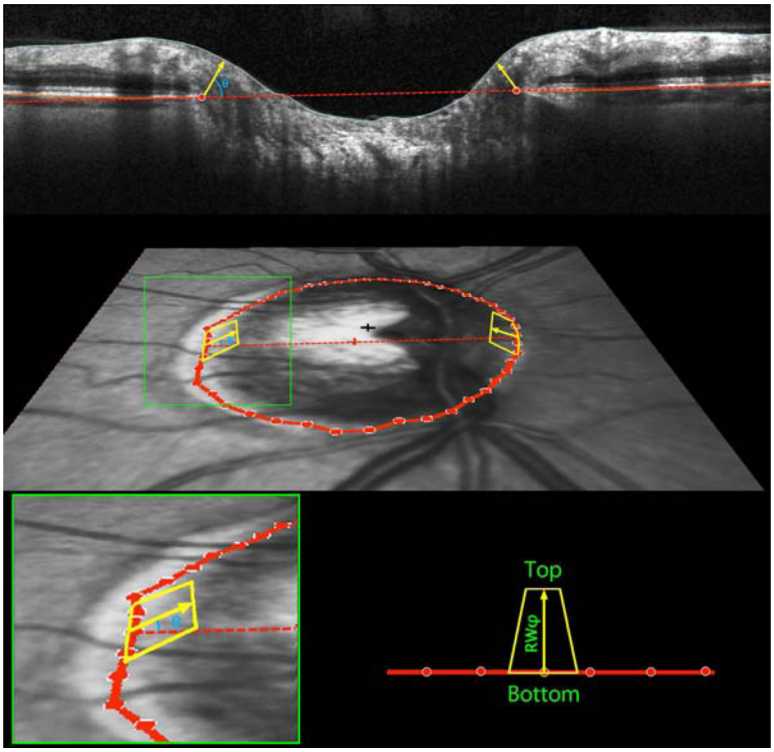

Figure 2. Definition and calculation of Bruch's Membrane Opening Minimum Rim Width and Minimum Rim Area, as used to Estimate the Amount of Neuroretinal Rim Tissue in Glaucoma

(Top) Within each of the 24 radial scans, Bruch's Membrane Opening was delineated (red circles). The minimum rim width within that sector was defined as the shortest distance from this point to the Inner Limiting Membrane (yellow arrow, at angle θ above the Bruch's Membrane Opening plane). These were averaged across sectors to give the global measure Bruch's Membrane Opening Minimum Rim Width. (Middle Panel) Within each sector, rim areas (yellow trapezoids) were calculated as the areas of trapezia at varying angles above Bruch's Membrane Opening plane. The height of each trapezium equals the rim width at this angle, referred to as RW_θ. The base equals the circumference within that sector, $2\pi r/48$, where r represents the distance from Bruch's Membrane Opening centroid (red cross). The top then has length $2\pi r / 48 \times (r - RW_\theta * \cos(\theta))$. (Bottom Panel) Within each sector the smallest such area was found, at angle ϕ, and its area calculated as (top+bottom)$\times RW_\phi/2$. Note that $RW\phi$ will not always be the minimum rim width within this sector, as illustrated in Supplementary Figure S1. The global measure BMO-MRA is generated by summing the areas of these 48 trapeziums.

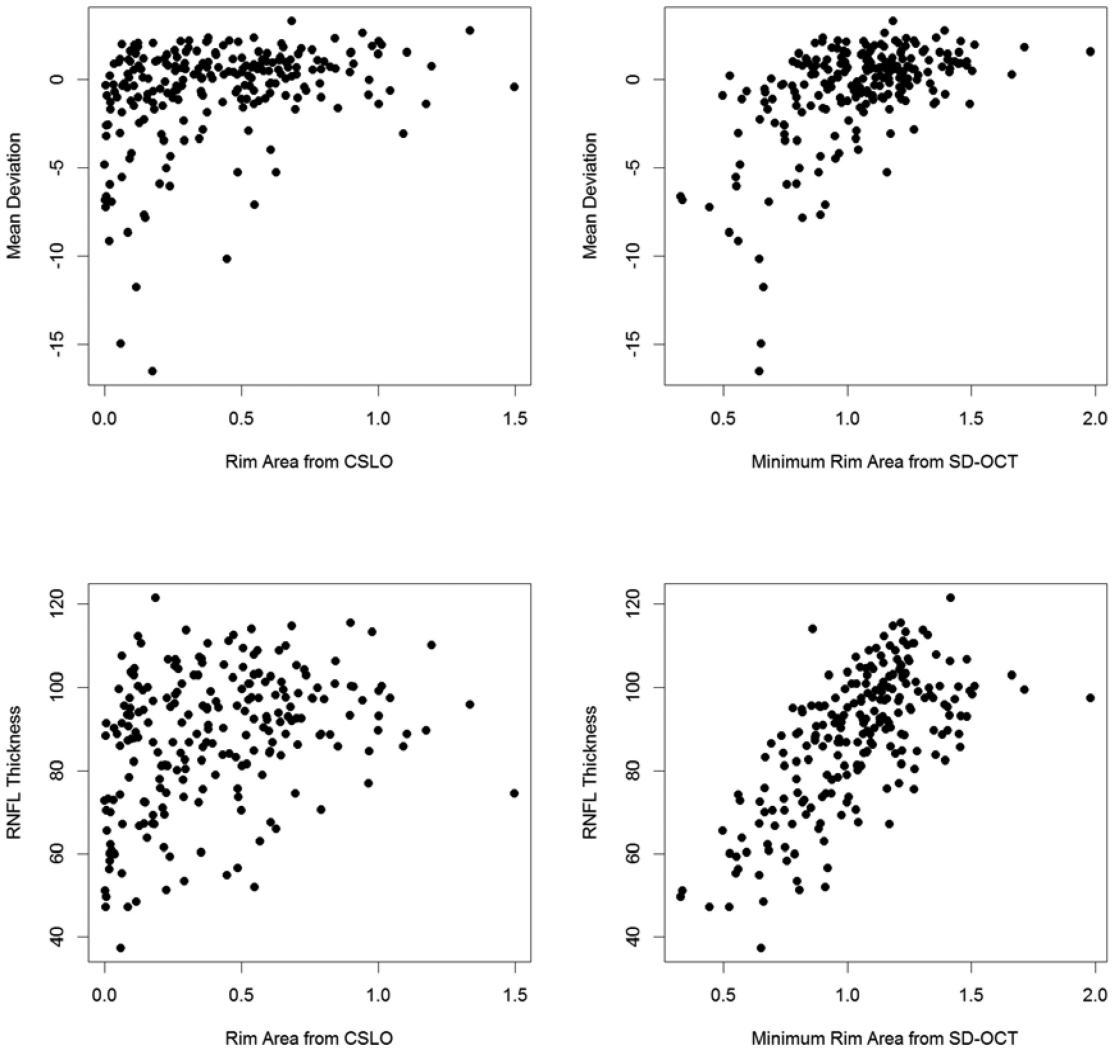

Figure 3. Relations between Two Estimates of the Amount of Neuroretinal Rim Tissue in Glaucoma and Either Mean Deviation from Perimetry or Retinal Nerve Fiber Layer Thickness

Mean Deviation (in dB) and RNFL thickness (from an SD-OCT peripapillary circle scan, in μm) are plotted against the Rim Area (in mm^2) as measured by Confocal Scanning Laser Ophthalmoscopy (CSLO), or the Bruch's Membrane Opening Minimum Rim Area from spectral domain optical coherence tomography (SD-OCT) based on the minimum distance between inner limiting membrane and Bruch's Membrane Opening.

Table 1

Characteristics of the 221 participants in a cohort used to assess measures of neuroretinal rim tissue.

	Mean	SD	Range
Age (years)	64.2	11.1	33.7 to 89.8
Intraocular Pressure (mmHg)	17.4	3.5	5.0 to 29.0
Mean Deviation (dB)	−0.69	2.90	−16.53 to 3.29
CSLT Rim Area (mm^2)	0.41	0.30	0.00 to 1.50
SD-OCT Horizontal Rim Area (mm^2)	1.25	0.35	0.34 to 2.63
SD-OCT Minimum Rim Width (μm)	250	66	75 to 389
SD-OCT Minimum Rim Area (mm^2)	1.04	0.26	0.33 to 1.98
SD-OCT RNFL thickness (μm)	87.8	16.2	37.5 to 121.4

Subject demographics are presented together with summaries of the measures of Retinal Nerve Fiber Layer (RNFL) thickness and Rim Area by Confocal Scanning Laser Tomography (CSLT) and spectral domain Optical Coherence Tomography (SD-OCT).

Table 2

Correlations between different measures of neuroretinal rim area and four outcome measures, in a cohort of 221 subjects.

	CSLT Rim Area	Horizontal Rim Area	Minimum Rim Width	Minimum Rim Area
MD	0.321	0.403	0.546	0.534
$MD_{1/C}$	0.294	0.343	0.489	0.471
$MD_{1/C}$(cap)	0.305	0.374	0.526	0.505
RNFL thickness	0.330	0.482	0.680	0.676

CSLT Rim Area represents the rim area from confocal scanning laser tomography; Horizontal Rim Area represents the rim area within the plane of Bruch's Membrane Opening using spectral domain optical coherence tomography (SD-OCT); Minimum Rim Width represents the width from Bruch's Membrane Opening to the Inner Limiting Membrane, tangentially perpendicular, using SD-OCT, averaged across radial scans; Minimum Rim Area represents the minimum area from Bruch's Membrane Opening to the Inner Limiting Membrane from SD-OCT, summed across sectors as defined by the radial scans. MD represents the Mean Deviation from perimetry in dB; $MD_{1/C}$ represents the average total deviation expressed on a scale that is proportional to 1/Contrast; $MD_{1/C}$(cap) is calculated the same as $MD_{1/C}$ but after capping all total deviation values at zero to reduce variability; and RNFL thickness represents the average peripapillary retinal nerve fiber layer thickness as measured by OCT.